Available online at www.sciencedirect.com

ScienceDirect

Ceramics International 40 (2014) 1037–1043

CERAMICS INTERNATIONAL

www.elsevier.com/locate/ceramint

Fabrication of Ni/WC composite with two distinct layers through centrifugal infiltration combined with a thermite reaction

Yu Xu[a], Zengchao Yang[a], Zhao Han[b,c], Guanghua Liu[c], Jiangtao Li[c,*]

[a]*School of Materials Science and Engineering, University of Science and Technology Beijing, Beijing 100083, PR China*
[b]*School of Metallurgy and Resources, Anhui University of Technology, Ma'anshan 243002, PR China*
[c]*Technical Institute of Physics and Chemistry, Chinese Academy of Sciences, Beijing 100190, PR China*

Received 26 March 2013; received in revised form 18 June 2013; accepted 27 June 2013
Available online 3 July 2013

Abstract

A simple and energy-efficient method combining a thermite reaction and centrifugal infiltration was applied to produce Ni/WC composites. Driven by a centrifugal force, the molten Ni in-situ produced by a thermite reaction infiltrated into a porous preform of WC powder compact. After solidification, a Ni/WC composite was obtained with two metallurgically bonded layers. Both of the two layers were composed of Ni and WC but with different contents. In different regions of the sample, WC particles with different morphologies and sizes were observed, which were caused by the competition of growth and relaxation of WC particles. The WC-rich layer showed an average hardness of 81.5 HRA, and the hardness of the Ni-rich layer gradually decreased from 61.4 HRA to 53.9 HRA.

Keywords: A. Powders: solid state reaction; B. Composites; C. Hardness; D. Carbides

1. Introduction

Metal matrix composites (MMCs) have drawn wide attention since they combine both metal and ceramic phases and thus exhibit better wear resistance, higher specific elastic modulus and strength compared to monolithic metals. Magnesium-, aluminum-, titanium-, copper-, iron- and nickel-based MMCs have been well studied and have found wide applications in automotive, aerospace and electronic fields. For example, prominent wear and tribological properties have made MMCs promising candidates for applications with severe wear abrasive conditions [1].

Both solid-state and liquid-state routes have been used to fabricate MMCs [2]. For instance, powder metallurgy method belonging to the solid-state route is commonly used in the production of cemented carbides while the liquid-state route is primarily based on the casting technique and it has advantages in obtaining near-net-shape final products in a simple and cost-effective manner. Liquid infiltration is a kind of liquid-state route. When the liquid metal is poured into a mold where a porous preform made of reinforcements is placed in advance, it can infiltrate into the pores of the preform with the assistance of driving forces. After solidification, the metal matrix tightly bonds the reinforcements and a composite can be produced. According to the infiltration driving forces, liquid infiltration can be divided into spontaneous infiltration, squeeze casting and pressure-assisted casting [3]. However, by now, papers in terms of liquid infiltration are mainly about light metals such as magnesium, aluminum and titanium; also the iron-based composite is fabricated through infiltration because the casting technique for steel is pretty mature [4–6]. The common characteristic is that in all these cases, molten metals are prepared by melting ingots in an external furnace, which consumes a large amount of energy especially when the melting point of the metal is high and requires relatively complicated apparatuses and production processes.

Nickel-based MMCs reinforced by WC particles with different volume fractions have been intensively investigated. Cemented carbides with nickel as the binding phase have been regarded as promising partial or total substitutions of Co-based cemented carbides, since nickel is also a prominent ductile and

---

*Corresponding author. Tel.: +86 10 82543695.
E-mail addresses: ljt0012@vip.sina.com, ahxyu90@163.com (J. Li).

0272-8842/$ - see front matter © 2013 Elsevier Ltd and Techna Group S.r.l. All rights reserved.
http://dx.doi.org/10.1016/j.ceramint.2013.06.101

wetting phase to combine WC particles but is cheaper and more erosion-resistant than cobalt [7–9]. In addition, WC reinforced Ni surface composites [10–15] have also been produced by laser cladding, spray coating or electrodeposition to form wear-resistant layers on steel/copper substrates. It was found that as thick as 1 mm layers were successfully produced and were metallurgically bonded with the substrates and remarkably higher hardness could be obtained than that of the substrates. Consequently, better tribological and wear properties were gained in the surface-modified substrates than those unmodified. It should be noted that either Ni-based cemented carbides or surface composites were mainly fabricated through solid-state routes. To be more specific, the raw materials are mainly Ni and WC powders. To our knowledge, few results [16] about the production of a bulk Ni/WC composite through infiltration have ever been reported.

To avoid the drawbacks that a relatively high temperature is required for melting nickel alloys (the melting point of pure nickel is 1726 K) and complicated processes are necessary for melting and transfer of the molten nickel alloy [17], the primary idea of this work is to find a novel method to obtain liquid nickel and to infiltrate it into a WC preform simultaneously to produce a bulk Ni/WC composite. The thermite reaction provides the opportunity to acquire liquid nickel without any need of an external heating apparatus. As a form of oxidation–reduction reaction, the thermite reaction can be used to produce a mixture of ceramic (usually alumina) and metal (nickel, iron, chromium, etc.). Both ceramic and metal are in molten state on account of the high exothermic inherence of the thermite reaction which results in a reaction temperature significantly higher than the melting temperatures of both ceramic and metal. Under the action of centrifugal forces, molten ceramic and metal can be separated from each other due to the differences of density and surface tension between the constituents. In addition, through changing the value of centrifugal forces, the degree of separation can be controlled, which makes the fabrication of various materials possible [18]. In this study, a high-temperature mixture of molten alumina and nickel was generated and they were separated under a centrifugal field. Since the density of liquid nickel (8.9 g/cm^3) is pretty larger than that of alumina (3.97 g/cm^3), the molten nickel segregated toward the bottom of the mold which was at the outer periphery of the centrifugal apparatus. Preplaced loose WC particles were on the bottom of the mold and interstices among the particles were saturated by the liquid nickel during infiltration. After solidification, a bulk Ni/WC composite would be successfully fabricated.

2. Experimental

Commercial WC (purity ≥99.8%, ~4 μm), NiO (purity Ni≥77.8%, 15 μm) and Al (purity 99.9%, 100-mesh) powders were used as raw materials. According to the reaction equation (see Eq. (1)), the mass ratio of NiO to Al was determined to be 80:20. The mixed NiO–20 wt% Al powders were dry milled using zirconia balls in a PTFE mill for 1 h at a speed of 30 rpm and then were dried at a temperature of 120 °C for 5 h. Each batch of 50 g mixed powders was cold-pressed into a compact form with a uniaxial pressure of 10 MPa in a steel mold with an inner diameter of 40 mm. Five batches were placed together in a silica tube also with an inner diameter of 40 mm. Loose WC particles with a weight of 60 g (40 mm in diameter and 8.5 mm in thickness) were preplaced on the bottom of the tube. The silica tube and powders were thereafter placed in a graphite mold with an inner diameter of 50 mm, and the blank area between the outer periphery of the silica tube and the inner periphery of the graphite mold was filled by quartz sand for heat insulation. Then, the mold was coated by a carbon felt and was put into a steel vessel mounted on a Ni-based superalloy rotator. The rotator as well as other assemblies was placed in a closed reaction chamber. Schematic description is present in Fig. 1.

$$3\text{NiO}+2\text{Al}=3\text{Ni}+\text{Al}_2\text{O}_3,\ (\Delta H_\text{r}=-891.76\ \text{kJ/mol},\ T_\text{ad}=3524\ \text{K}) \quad (1)$$

The reaction chamber was evacuated to a vacuum of <100 Pa. Subsequently, the rotator was started. By changing the rotation speed, a high centrifugal field ranging from 100g to 5000g could be generated in a laboratory scale (g is the gravity acceleration). A tungsten coil was placed near the reactants and was used to ignite the thermite reaction after the rotation speed reached the designed value. A large amount of heat was generated and the reaction products, namely alumina and nickel, were both melted. Due to the density difference between alumina and nickel, separation of these two molten constituents occurred and the nickel then segregated towards the bottom of the mold and infiltrated into the interstices among the loose WC particles. A bulk Ni/WC composite was fabricated after solidification. Bulk alumina was also produced as a by-product. In this work, the value of the centrifugal field

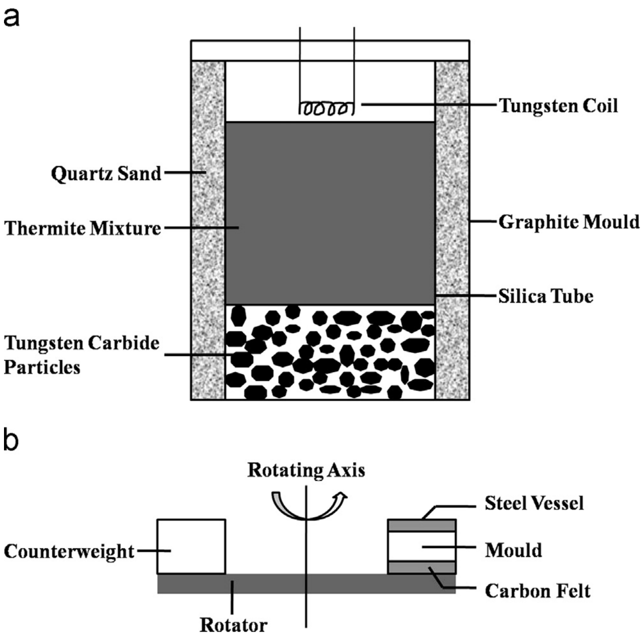

Fig. 1. Schematic descriptions of (a) mold and (b) rotating system.

was determined to be 500*g* which was sufficient enough to fully separate these two reaction products.

Specimen of the cross section of the composite was prepared by standard polishing techniques. The microstructure of the composite was examined by scanning electron microscopy (SEM; S-3400, Hitachi, Japan) equipped with an energy-dispersive X-ray spectrometer (EDS; INCA, Oxford Instrument, UK). X-ray diffraction (XRD; D8 Focus, Bruker, Germany) was used to identify the possible phases in the composite and a Rockwell hardness tester was also used to assess the hardness profile of the composite.

3. Results and discussion

3.1. Macrostructure of the sample

As shown in Fig. 2, a Ni/WC composite with bulk alumina as the byproduct was successfully fabricated through centrifugal infiltration combined with SHS reaction of the thermite composed of Al and NiO. After ignition, the mixed powders reacted violently in a self-propagating manner, and remarkable high temperature was generated. The molten alumina and nickel were separated from each other in a centrifugal field and the molten nickel infiltrated into the WC preform. Due to the decrease of temperature, thereafter both would solidify. The ultimate result of the separation, infiltration and solidification processes was two totally separated layers, namely cylindrical bulk alumina (40 mm in diameter, 10 mm in thickness and a weight of 21.07*g*) on the upper layer and a cylindrical composite ingot (40 mm in diameter, 14 mm in thickness and a weight of 173.83*g*) on the lower layer.

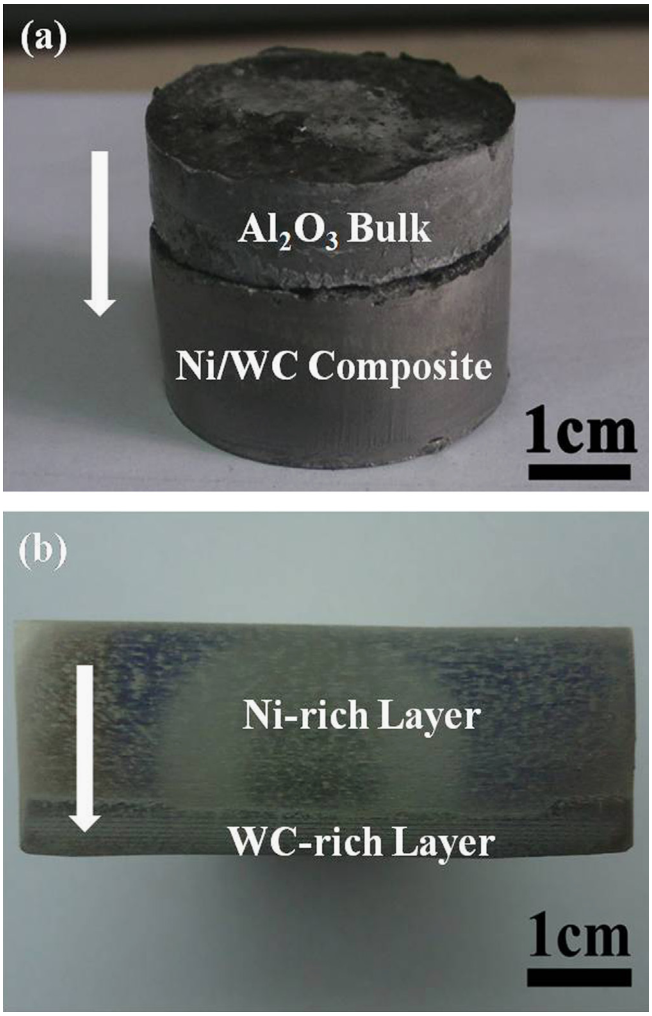

Fig. 2. (a) The macrostructure of the products and (b) the cross-section of the Ni/WC composite which shows two different layers. The white arrow indicates the direction of centrifugal forces.

Fig. 2(b) shows the cross section of the Ni/WC composite. Two closely adherent layers with different colors can be observed. Along the direction of centrifugal forces, the upper layer with light color is enriched in Ni, whereas the lower layer with darker color is enriched in WC. It is obvious that the thickness of the WC-rich layer is remarkably smaller than the initial thickness of the preplaced loose WC particles, which are 4 mm and 8.5 mm respectively. This can be explained by densification of loose WC particles during the centrifugal process as well as the transfer of WC particles. Before and after the thermite mixture was ignited, substances above the preform were solid particles and liquid mixture respectively. Undoubtedly, both could generate a high pressure (about mg'/S, m is the mass value, g' is the centrifugal acceleration and S area of the cross section of the preform) on the preform. For instance, before ignition, the thermite mixture generated a pressure which was calculated to be as high as 0.97 MPa on the surface of the preform, and it certainly packed the loose WC particles and thus densified the preform. During the liquid nickel infiltration of the preform, relocation of WC particles also occurs since the liquid flow would carry the WC particles with itself. In addition, according to the previous report [19], the thermite reaction is characterized by ejection due to the formation of lower aluminum oxides vapors in the combustion front and the evaporation of impurity gases. The ejection resulted in deformation of loose WC particles preform which was weak in strength. Another consequence of the ejection was the presence of WC particles in the upper Ni-rich layer, which would be discussed in the following part. In conclusion, densification of the preform, relocation of WC particles and the ejection of the thermite reaction contribute to the decrease in thickness of the WC-rich layer.

Former reports [20] on the thermite reaction in a centrifugal field generally proposed that the reaction was accompanied by interfacial separation of the metallic and oxide molten products. The infiltration of metallic phase into the lower porous layer followed the separation. In this paper, the lower layer was porous preform composed of loose WC particles. Because the WC particles were restricted in the tube and have the largest density, large amounts of WC particles still stayed within the preform. The produced Ni melt would infiltrate into the preform until the pores were fully saturated. Since the amount of Ni melt was larger than that needed to attain a full saturation, the remained Ni would form an overlying layer on the preform. After solidification, a bulk composite with two metallurgically bonded layers would be obtained.

3.2. *Results of X-ray analysis of the composite*

Possible phases in the composite were identified by X-ray diffraction. The results are shown in Fig. 3. Only WC and Ni phases exist in both WC-rich layer (a) and Ni-rich layer (b). Undoubtedly, the WC phase in the WC-rich layer originates from the preplaced WC particles whilst the WC phase in the Ni-rich layer comes from the deformation of the weak preform due to ejection of the thermite reaction. The ejection resulted in the transfer of WC particles to the upper layer; fine particles in particular considering their movement were less hindered than that of coarse particles. The observed Ni in both the two layers is the product of the thermite reaction. The produced Ni melt would infiltrate into the pores of the WC preform, which is controlled by the centrifugal forces. Besides, the frequently observed brittle intermetallic compounds Al_3Ni and Al_3Ni_2 in Al–Ni system are not observed either. According to the Al–Ni binary phase diagram, the formation of Al_3Ni is at $T < 1128$ K while Al_3Ni_2 is at $1128\ \text{K} < T < 1406$ K [21]. Considering that the adiabatic temperature of Al–NiO system is 3524 K [18] and the real reaction temperature of this system can be as high as 3013 K [19], it is reasonable that no nickel aluminides formed.

3.3. *Microstructure of the composite*

Microstructure observation was done with a specimen machined from the bulk Ni/WC composite on the plane parallel to the rotating plane along the direction of centrifugal forces. Results are present in Fig. 4. On the whole, two layers and the transition area are dense, as few pores are observed. Clearly, constitution, microstructure and morphology as well as size of WC particles vary with location.

By selecting several different areas in a certain layer under a relatively low magnification to do the EDS scanning, values of constitution of the two layers and the transition area were obtained. Since the content of the carbon element was difficult to be detected accurately, only data of nickel and tungsten elements were used to evaluate the constitution. Results are present in Table 1. It should be noted that overall values of contents of nickel and tungsten elements have been normalized. Apparently, both contents of nickel and tungsten (reflecting the content of WC) vary along the direction of centrifugal forces. The content of WC increases significantly from the Ni-rich layer to the WC-rich layer, which may result in a gradation in properties.

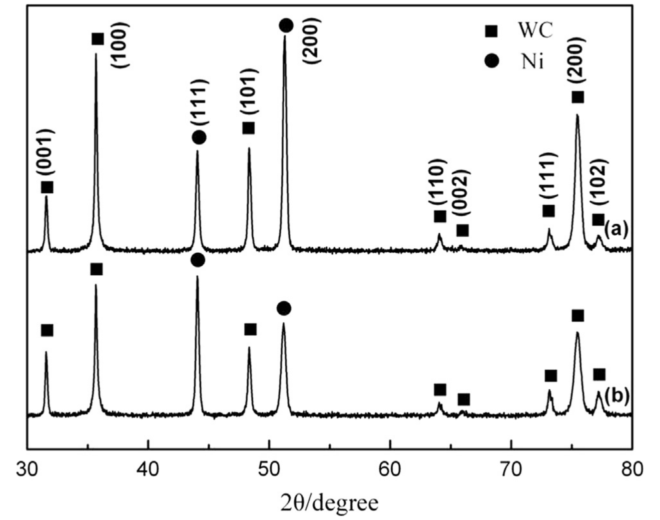

Fig. 3. XRD patterns of the as-prepared Ni/WC composite: (a) WC-rich layer and (b) Ni-rich layer.

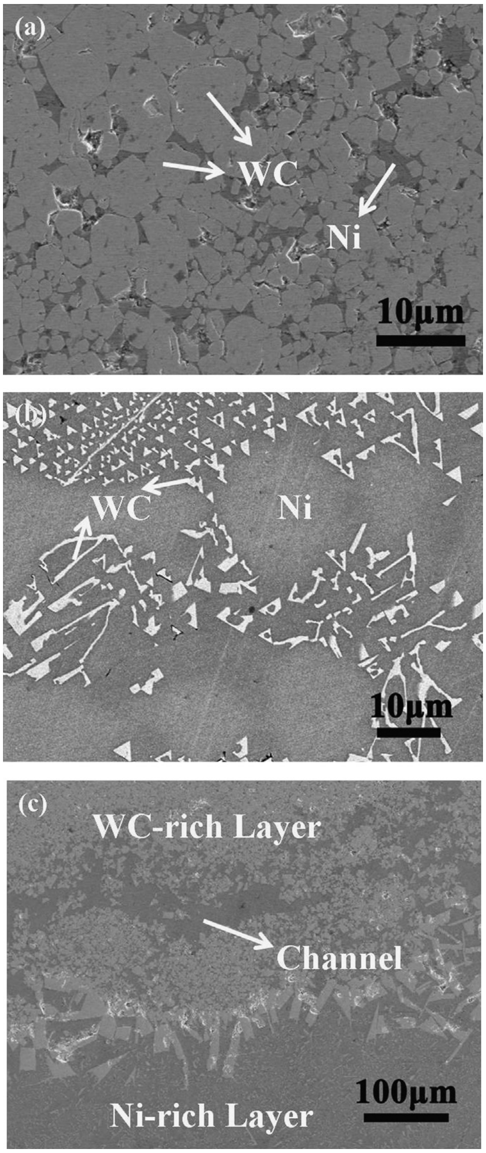

Fig. 4. SEM photographs of the composite: (a) WC-rich layer, (b) Ni-rich layer and (c) transition area.

In the WC-rich layer (see Fig. 4(a)), granular WC particles are distributed homogeneously and tightly bonded with the nickel phase. According to the structure formation process proposed, the molten nickel was separated from the molten mixture and then infiltrated into the interstices among the WC particles under the centrifugal forces. The molten nickel flowed among the WC particles, solidified with the decrease of temperature and was finely bonded with the WC particles on

Table 1
Constitution within the two layers and the transition area.

		WC-rich layer	Transition area	Ni-rich layer
Ni	Weight%	16.4	31.2	56.5
	Atomic%	37.9	58.7	80.3
W	Weight%	83.6	68.8	43.5
	Atomic%	62.1	41.3	19.7

account of the good wettability between them. It is obvious that in this layer the WC particles account for a significantly large proportion and thus can be regarded as the major phase. Growth of WC particles seems to have taken place since size of particles ranges from 2 μm to 10 μm according to the results, whereas the primary used WC particles are around 4 μm in size.

As mentioned earlier, ejection of the thermite reaction caused the transfer of WC particles to the Ni-rich layer, which is demonstrated by the SEM result (see Fig. 4(b)). Under the action of centrifugal forces, displaced WC particles in fact could settle due to their larger density than that of molten mixture of reaction products. However, if a large amount of WC particles were displaced and viscosity of the molten mixture increased rapidly as the temperature decreased, some WC particles would remain in the Ni-rich layer and get agglomerated in certain areas. Two morphologies of WC particles can be observed, i.e. triangle and strip-like shape, which are both completely different from that of the starting WC particles.

Fig. 4(c) shows the microstructure of the transition area. Pores are rarely observed and the Ni-rich and WC-rich layers are tightly bonded. Near the Ni-rich layer, elongated rectangular-shape WC particles with a length as large as 50 μm are observed. Whilst near the WC-rich layer, WC particles are still in a granular shape. In addition, near the WC-rich layer, channels which are enriched in nickel occur. This may be caused by the deformation of loose WC particles preform during the centrifugal infiltration process, which was also observed in other research works [3,22] on the production of MMCs by centrifugal infiltration.

3.4. Characteristic of WC particles

In SEM photographs of the unetched specimen previously discussed, variations in shape and size of WC particles have been referred to. In previous studies, such variations of WC particles in liquid phase sintering of WC-based cemented carbides have also been reported [23–25], which is important for the optimization of microstructure of the material. Since the temperature during the thermite reaction and subsequent infiltration is remarkably higher than sintering temperature, such a phenomenon seems to be inevitable. It was also found in Ref. [19].

In order to identify the variations of morphology and size of WC particles, an etched specimen was studied. Results are present in Fig. 5. The primarily used WC particles are in a granular shape with a size ranging from 2 μm to 5 μm and small particles agglomerate around large ones, which are shown in Fig. 5(a). In the WC-rich layer (see Fig. 5(b)), some WC particles increase in size to about 10 μm but still retain their initial morphology. Grain boundaries are also observed between two WC particles. Whilst in the Ni-rich layer (see Fig. 5(c)), the shape of WC particles is completely different from that of starting powders. Two "types" of WC particles observed in the unetched specimen (see Fig. 4(b)) are as a matter of fact in the same shape, i.e. a well-developed triangular prism shape. However, these triangular-prism-shape WC particles are arranged in different directions, namely with the prism plane perpendicular or parallel to the direction of centrifugal forces. When it comes to the transition area (see Fig. 5(d)), WC particles are observed to be in an elongated rectangular shape (the prismatic plane of the WC particle). These particles distribute randomly with a size as large as 60 μm.

According to [23], recrystallization of WC particles in a liquid phase sintering process results in WC particles having two kinds of shape, namely an equilibrium shape and a growth-determined shape. The WC crystal is hexagonal and is formed by two families of planes (i.e. basal $\{0001\}$ planes and prismatic $\{10\bar{1}0\}$ planes) with different interfacial properties (energy and growth rate). Therefore, a well-developed WC grain is in a triangular prism shape. Both the relaxation process and the growth process proceed in three steps, namely dissolution, diffusion and subsequently reprecipitation. When diffused WC atoms reprecipitate on the same carbide grain, the process is called relaxation, leading to an equilibrium shape; if diffused atoms reprecipitate on another grain, it is called growth, leading to a growth-determined shape. Ratio of values of the diffusion flux in relaxation (j_r) and growth (j_g) process j_r/j_g is calculated to be proportional to λ/d_{WC}, where λ is the mean linear path in the liquid phase and d_{WC} the WC grain size [23].

In this paper, formation of the different morphologies of WC particles in the WC-rich layer and the Ni-rich layer can be well explained by a growth-determined and a relaxation-determined process respectively. Since the content of nickel in the WC-rich layer is relatively low, the ratio of the mean linear intercept of the nickel binder phase to the carbide crystal size is relatively small, resulting in a larger diffusion flux of growth (j_g) than that of relaxation (j_r). Thus, the WC particles witnessed an increase in size while retaining their initial shape to a certain degree. However, existence of WC particles in the Ni-rich layer was caused by ejection during the thermite reaction which results in the transfer of WC particles. Also, fine powders were more likely to be transferred since their displacement was less hindered. According to Stokes' Law, the coarser the displaced particles, the larger the velocity of settlement of WC particles under the action of centrifugal forces. Consequently, displaced particles remaining in the Ni-rich layer are relatively fine, while at the same time this layer is enriched in nickel phase. Therefore, j_g/j_r is smaller than 1 and the relaxation process predominates the recrystallization of WC grains, resulting in a near-equilibrium shape, i.e. the triangular prism shape.

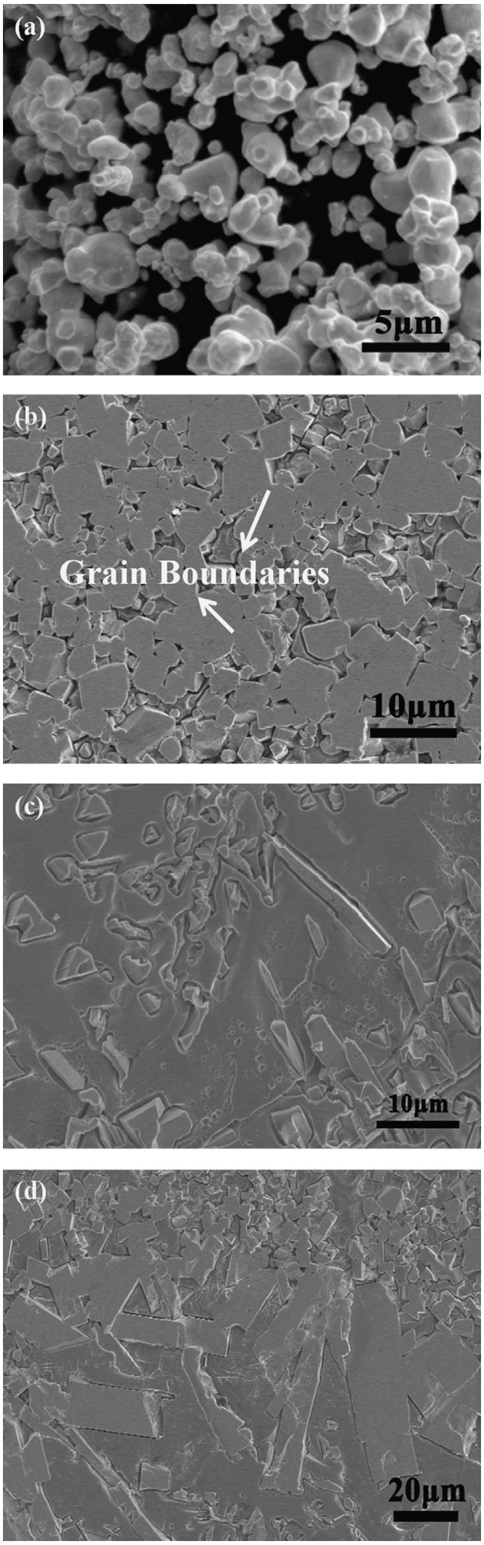

Fig. 5. Morphologies of WC particles in (a) starting materials, (b) WC-rich layer, (c) Ni-rich layer and (d) transition area.

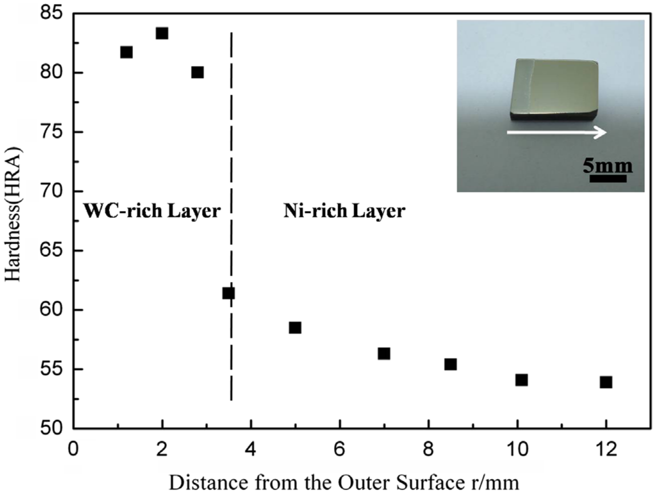

Fig. 6. Hardness profile of the Ni/WC composite. The white arrow indicates the direction from the outer to the inner surface of the composite. The dotted line shows the position of the boundary of these two layers.

WC particles in the transition area underwent both apparent variation in shape and growth in size. As already known, in conventional centrifugal casting, the solidification front propagates from the outer periphery to the inner periphery of the mold. Therefore, compared with the WC-rich layer, the transition area could maintain the liquid state for a long time, which is beneficial for the diffusion of carbide atoms. In addition, interactions among WC particles in the transition area were relatively weak, leading to less hindering of growth of particles by neighboring ones. These two factors contributed to the significant growth in size of WC particles within the transition area. While in comparison with the Ni-rich layer, the transition area had a higher concentration of atoms, which means the absolute value of j_r was relatively large. Relaxation process occurred and the morphology of WC particles shifted to a near-equilibrium shape. In conclusion, the ultimate shape and size of WC particles in the transition area are balanced by both the growth-determined and relaxation processes.

3.5. Hardness profile of the Ni/WC composite

Macrohardness was measured by the Rockwell hardness test with a polished specimen on the plane perpendicular to the rotating axis. Results are presented in Fig. 6 showing that the value of hardness varies along the direction of centrifugal forces. Hardness as high as 83.3 HRA is obtained in the WC-rich layer with a thickness of about 3.5 mm, whereas moving to the inner surface of the composite, the hardness dramatically decreases from an average 81.5 HRA in the WC-rich layer to about 61.4 HRA in the transition area, and further smoothly diminishes within the Ni-rich layer, where the smallest value of hardness is 53.9 HRA. High hardness in the WC-rich layer is because of the presence of large amounts of WC particles. Since the concentration of WC in the Ni-rich layer is relatively low, it is reasonable that hardness in this layer is lesser than that in the WC-rich layer.

4. Conclusion

A thermite reaction was combined with centrifugal infiltration to produce a bulk Ni/WC composite. The as-prepared Ni/WC composite was composed of two metallurgically bonded layers, namely a Ni-rich layer and a WC-rich layer. WC particles were found to be different in both morphology and size in different areas. In the Ni-rich layer, WC particles showed a near-equilibrium shape because of relaxation of WC. In the WC-rich layer, the size of WC particles increased due to the growth of WC. In the transition area between the two layers, the size and morphology of WC were controlled by the balance of growth and relaxation. The hardness of the composite was location-dependent. The Rockwell hardness of the WC-rich layer reached 83.3 HRA, while in the Ni-rich layer the hardness gradually decreased from 61.4 HRA to 53.9 HRA.

Acknowledgments

This work is supported by National Natural Science Foundation of China (Grant nos. 50932006, 51002163, and 51001111), National Magnetic Confinement Fusion Science Program (Code nos. 2010GB106000 and 2010GB106003), Beijing Natural Science Foundation (Grant no. 2112043), and Key Laboratory of Functional Crystals and Laser Technology, TIPC, CAS.

References

[1] J.W. Kaczmar, K. Pietrzak, W. Wlosinski, The production and application of metal matrix composite materials, Journal of Materials Processing Technology 106 (2000) 58–67.
[2] M. Rosso, Ceramic and metal matrix composites: routes and properties, Journal of Materials Processing Technology 175 (2006) 364–375.
[3] Jessada Wannasin, Centrifugal Infiltration of Particulate Metal Matrix Composites: Process Development and Fundamental Studies, Ph.D. Thesis, Massachusetts Institute of Technology, June 2004.
[4] Rong Zhou, Yehua Jiang, Dehong Lu, The effect of volume fraction of WC particles on erosion resistance of WC reinforced iron matrix surface composites, Wear 255 (2003) 134–138.
[5] Yoshinori Nishida, Itaru Shirayanagi, Yoshibumi Sakai, Infiltration of fibrous preform by molten aluminum in a centrifugal force field, Metallurgical and Materials Transactions A 27 (1996) 4163–4169.
[6] Mohamed A. Taha, Nahed A. El-Mahallawy, Metal–matrix composites fabricated by pressure-assisted infiltration of loose ceramic powder, Journal of Materials Processing Technology 73 (1998) 139–146.
[7] Guojian Jiang, Wenlan Li, Hanrui Zhuang, Synthesis of tungsten carbide–nickel composites by the field-activated combustion method, Materials Science and Engineering A 354 (2003) 351–357.
[8] Hwan-Cheol Kim, In-Jin Shon, Jin-Kook Yoon, Jung-Mann Doh, Z.A. Munir, Rapid sintering of ultrafine WC–Ni cermets, International Journal of Refractory Metals and Hard Materials 24 (2006) 427–431.
[9] Hongsheng Chen, Keqin Feng, Ji Xiong, Jianjun Luo, Zhixing Guo, Hui Wang, Characterization and forming process of a functionally graded WC–Co/Ni composite, International Journal of Refractory Metals and Hard Materials 35 (2012) 306–310.
[10] Shengfeng Zhou, Yongjun Huang, Xiaoyan Zeng, Qianwu Hu, Microstructure characteristics of Ni-based WC composite coatings by laser induction hybrid rapid cladding, Materials Science and Engineering A 480 (2008) 564–572.
[11] M. Stroumbouli, P. Gyftou, E.A. Pavlatou, N. Spyrellis, Codeposition of ultrafine WC particles in Ni matrix composite electrocoatings, Surface and Coatings Technology 195 (2005) 325–332.
[12] M. Surender, B. Basu, R. Balasubramaniam, Wear characterization of electrodeposited Ni–WC composite coatings, Tribology International 37 (2004) 743–749.
[13] Y. Wang, Z. Xu, Nanostructured Ni–WC–Co composite coatings fabricated by electrophoretic deposition, Surface and Coatings Technology 200 (2006) 3896–3902.
[14] M.M. Stack, D. Pena, Particle size effects on the elevated temperature erosion behaviour of Ni–Cr/WC MMC-based coatings, Surface and Coatings Technology 113 (1999) 5–12.
[15] Chen Zhenda, Lim Leong Chew, Qian Ming, Laser cladding of WC/Ni composite, Journal of Materials Processing Technology 62 (1996) 321–323.
[16] R. Subramanian, J.H. Schneibel, Intermetallic bonded WC-based cermets by pressure melt infiltration, Intermetallics 5 (1997) 401–408.
[17] Zong-de Liu, Juan Tian, Bin Li, Li-ping Zhao, Microstructure and mechanical behaviors of in situ TiC particulates reinforced Ni matrix composites, Materials Science and Engineering A 527 (2010) 3898–3903.
[18] L.L. Wang, Z.A. Munir, Y.M. Maximov, Review. Thermite reactions: their utilization in the synthesis and processing of materials, Journal of Materials Science 28 (1993) 3693–3708.
[19] V.N. Sanin, V.I. Yukhvid, A.E. Sychev, N.V. Sachkova, M. Yu Shiryaeva, The effect of microgravity on the composition of SHS products of the mixture NiO+Ni+Al+WC, Inorganic Materials 45 (2009) 635–644.
[20] V.N. Sanin, V.I. Yukhvid, Centrifugation-driven melt infiltration in high-temperature layered systems, Inorganic Materials 41 (2005) 247–254.
[21] N. Sobczak, J. Oblakowski, R. Nowak, A. Kudyba, W Radziwill, Interaction between liquid aluminum and NiO single crystals, Journal of Materials Science 40 (2005) 2313–2318.
[22] J. Wannasin, M.C. Flemings, Fabrication of metal matrix composites by a high-pressure centrifugal infiltration process, Journal of Materials Processing Technology 169 (2005) 143–149.
[23] A.V. Shatov, S.A. Firstov, I.V. Shatova, The shape of WC crystals in cemented carbides, Materials Science and Engineering A 242 (1998) 7–14.
[24] Jong-Dae Kim, Suk-Joong L. Kang, Formation of grain boundaries in liquid-phase-sintered WC–Co alloys, Journal of the American Ceramic Society 88 (2005) 500–503.
[25] Sona Kim, Seok-Hee Han, Jong-Ku Park, Hyoun-Ee Kim, Variation of WC grain shape with carbon content in the WC–Co alloys during liquid-phase sintering, Scripta Materialia 48 (2003) 635–639.